JOURNAL OF SCIENCE AND TECHNOLOGY
ISSN: 2229-8460 e-ISSN: 2600-7924

JST

Vol. 17 No. 2 (2025) 64-83
https://publisher.uthm.edu.my/ojs/index.php/jst

Investigation of Prunus Domestica Leaves Aqueous Extracts as a Sustainable Solution for Corrosion Control of Carbon Steel in 1M HCl: Thermodynamic, Adsorption and Electrochemical Insights

Nikolay Akatyev[1]*, Meryuet Khapiyeva[1], Roza Kenzhegalieva[1], Aruzhan Talapova[1], Gaukhar Uzakbay[1], Aikorkem Tlektes[1], Alexandra Logashkina[1]

[1] *Faculty of Natural and Geographical Sciences,*
M. Utemisov West Kazakhstan University, Nazarbayev Ave. 162, Uralsk, 090000, KAZAKHSTAN

*Corresponding Author: n.akatyev.science@gmail.com
DOI: https://doi.org/10.30880/jst.2025.17.02.006

Article Info

Received: 14 April 2025
Accepted: 24 October 2025
Available online: 30 December 2025

Keywords

Plant extracts, inhibition efficiency, “green” inhibitors; carbon steel, metal protection, adsorption

Abstract

This study investigates the efficacy of Prunus domestica leaves aqueous extract (PDLAE) as a sustainable corrosion inhibitor for carbon steel in 1M hydrochloric acid solution. The research aligns with green chemistry principles, addressing the environmental concerns associated with the use of synthetic inhibitors. Comprehensive analyses, including weight loss assays, electrochemical measurements, adsorption isotherms, contact angle determination, and UV-visible spectroscopy, were conducted to evaluate the extract's corrosion inhibiting performance. The results revealed that the extract achieved a maximum inhibition efficiency of 92.07% at 2.0 g·dm^{-3} concentration after 24 hours, with thermally stable adsorption observed at high temperatures. Adsorption obeys the Langmuir model, indicating monolayer formation, and negative Gibbs free energy values (ΔG0ads > -20 kJ·mol-1) confirm spontaneous adsorption. Electrochemical tests demonstrated mixed-type inhibition behavior, reducing corrosion current density and enhancing charge transfer resistance. Additionally, the extract improved surface hydrophobicity, as evidenced by increased contact angles. FTIR analysis identified the presence of key phytoconstituents bearing hydroxyl and carbonyl functional groups and aromatic structures that contribute to corrosion inhibition efficiency. Obtained results highlight the PDLAE's potential as an eco-friendly and effective solution for metal protection and the importance of plant-based inhibitors in advancing environmentally benign corrosion prevention strategies.

1. Introduction

The growing emphasis on sustainable and environmentally friendly practices has driven significant interest in "green" chemistry, particularly in the development of eco-friendly corrosion inhibitors. Traditional corrosion inhibitors are often based on the synthetic chemicals that pose environmental and health risks, necessitating the search for safer, biodegradable alternatives. Plant extracts have emerged as the most promising candidates for this purpose due to their natural abundance, low toxicity, and rich phytochemical composition, which allow them to exhibit strong adsorption and protective properties on metal surfaces [1].

Prunus domestica (commonly known as the European plum) (Fig. 1) is a versatile plant with significant applications across various fields, reflecting its nutritional, medicinal, cosmetic, and environmental importance.

(a) **(b)**

Fig. 1 *European plum (Prunus domestica L.) (a) Whole plant*; *(b) Leaves*

The fruits of *P. domestica* are widely consumed fresh, dried, or processed into juices, jams, and desserts. They are rich in dietary fiber, vitamins (e.g., C and K), and minerals like potassium, contributing to digestive health and overall nutrition. Additionally, their high polyphenol content provides antioxidant benefits, which may help prevent oxidative stress-related diseases [2]. *P. domestica* fruits and extracts are recognized for their antioxidant, anti-inflammatory, and laxative properties. They are used in traditional and modern medicine to support gut health, regulate blood sugar levels, and reduce oxidative stress. Recent studies also highlight their potential in managing hypertension, diabetes, and liver health [3]. *P. domestica* seed oil and leaf extracts are increasingly utilized in skincare products for their moisturizing, anti-ageing, and antioxidant properties [4]. *P. domestica* trees are cultivated for their adaptability and role in agroforestry systems. They contribute to soil conservation and are explored for their genetic diversity in breeding programs. Additionally, their by-products are being studied for bioactive compounds with potential applications in green chemistry [5].

In this context, the leaves of *P. domestica* represent a potential source of natural corrosion inhibitors. These leaves are known to contain various phytochemicals with antioxidant and chelating properties, making them suitable for mitigating metal corrosion in an eco-friendly manner.

Nowadays, there are several known examples of the use of *P. domestica* extracts as corrosion inhibitors. Abd-El-Nabey *et al.* investigated the use of *P. domestica* seed extracts as eco-friendly corrosion inhibitors for steel in acidic environments. The results demonstrated significant inhibition efficiency, highlighting the potential of these extracts in green chemistry applications [6]. Kamran *et al.* developed a composite material using *P. domestica* gum grafted onto polyaniline (PDG-g-PANI) for corrosion protection of mild and stainless steel. The composite exhibited high corrosion inhibition efficiency (up to 99%) in both NaCl and H_2SO_4 environments, demonstrating the effectiveness of *P. domestica*-based materials in harsh conditions [7]. *P. domestica* extracts were also tested as corrosion inhibitors for aluminum alloy (AA6063-T5) in sodium chloride media. The study reported an inhibition efficiency of 99.01%, confirming the extract's suitability as a natural, non-toxic corrosion inhibitor [8].

In this case, our study explores the inhibition efficiency of PDLAE in a 1M hydrochloric acid solution, focusing on its adsorption behavior and protective mechanisms. By aligning with the principles of green chemistry, this research aims to contribute to the development of sustainable solutions for corrosion control, reducing the environmental footprint of industrial processes.

2. Materials and Methods

2.1 Reagents and Solvents

All analytical-grade reagents were used without any further purification. Double-distilled water (DDW) was used for the extraction and preparation of the corrosion media.

2.1.1 Plant Collection

The *P. domestica* leaves were collected in their natural habitat in the summer, away from highways and factories. Plant species were verified in the herbarium of M. Utemisov West Kazakhstan University's Faculty of Natural and

Geographical Sciences. The samples were thoroughly washed with tap water and DDW and kept in a shaded place to total dryness (approx. 2 weeks). After being dried, the samples were ground into a fine powder, sieved through a 1.0 mm sieve, and kept at 4°C until further use.

2.1.2 Preparation of the Extract

10 g of dried and ground plant material were transferred to a 250 ml Erlenmeyer flask and extracted 3 times with 100 ml of DDW in a water bath at 60°C for 8 hours. The temperature was maintained using a TW-2.02 water thermostat with an accuracy of ±0.1°C. The obtained extracts were combined and evaporated. The solid residue was dried at 50°C to constant weight and stored in dark sealed vials at 4°C and used for subsequent anticorrosion tests.

2.1.3 Metal Preparation

Carbon steel specimens used for corrosion tests, containing (wt. %) 97.8 – Fe; 0.22 – C; 0.65 – Mn; 0.30 – Si; 0.04 – P; 0.05 – S; 0.30 – Cr; 0.30 – Ni; 0.30 – Cu; 0.01 – N, with dimensions of 25.0×35.0×3.0 mm, were purchased from the industry. Before the experiment, the specimen was polished in sequence using emery paper with grit numbers from 250 to 1200. The specimens were washed in running water and DDW to remove oxides and dust and then cleaned and degreased with ethanol and acetone. The specimens were prepared and kept in a desiccator with silica gel until the upcoming corrosion tests.

2.2 Weight Loss (Gravimetric) Method

Weight loss experiments were performed to evaluate the corrosion rate (CR), inhibition efficiency (IE%), and degree of surface coverage (θ). Each coupon was immersed in an open-to-air 150 ml beaker containing 100 ml of corrosion medium at room temperature. After the specified immersion time, coupons were withdrawn from the beaker and washed in running water and DDW, and residues of corrosion products were removed by washing each coupon in a solution containing 50% NaOH and 100 g of zinc dust [9]. Then, coupons were again washed in running water and DDW, rinsed in ethanol and acetone, and dried in air before reweighting. All weight measurements were performed using an Ohaus Adventurer Pro AV264 analytical balance with an accuracy of ±0.1 mg.

The corrosion rate (CR g·m^{-2}·h^{-1}), inhibition efficiency (IE$_{wl}$%), and degree of surface coverage (θ) were calculated according to the following Equations (1–3), respectively:

$$CR(g \cdot m^{-2} \cdot h^{-1}) = \frac{\Delta m}{S \cdot \tau} \quad (1)$$

$$IE_{wl}(\%) = \frac{CR_0 - CR_i}{CR_0} \cdot 100 \quad (2)$$

$$\theta = \frac{IE_{wl}(\%)}{100} \quad (3)$$

Where Δm is the weight loss of the coupon (mg) after the immersion period (h), S is the surface area of the specimen (m^2), CR_0 is the corrosion rate of carbon steel without inhibitor, and CR_i is the corrosion rate of carbon steel in the presence of the inhibitor.

2.3 Activation Parameters Calculations

The activation energy was determined in accordance with the logarithmic form of the Arrhenius equation as follows:

$$logCR = log\ A - \frac{E_a}{2.303RT} \quad (4)$$

Where A is the Arrhenius pre-exponential factor, T – absolute temperature (K), and R – the universal gas constant (8.314 J·mol^{-1}·K^{-1}). The plots of logCR against 1/2,303RT exhibit as straight lines with the slope corresponding to E_a and the intercept to logA.

Enthalpy (ΔH*, kJ·mol^{-1}) and entropy (ΔS*, J·mol^{-1}·K^{-1}) of activation were obtained from the slope – ΔH*/2.303R and intercept [logR/Nh + (ΔS*/2.303R)], respectively, from the plot of logCR/T versus 1/T in accordance with the following alternative form of Arrhenius equation (5):

$$log\frac{CR}{T} = \frac{-\Delta H^*}{2.303RT}\left(\frac{1}{T}\right) + \left[log\frac{R}{N_A h} + \left(\frac{\Delta S^*}{2.303R}\right)\right] \quad (5)$$

Where h signifies Planck's constant, N_A denotes Avogadro's number, CR is the corrosion rate, T represents thermodynamic temperature, R denotes the universal gas constant, ΔS* is the entropy change, and ΔH* signifies the enthalpy change [10].

2.4 Absorption and Thermodynamics

The Langmuir, Temkin, Frumkin, Freundlich, Flory-Huggins, and El-Awady adsorption models were used to estimate the efficiency and nature of the inhibitor's interaction with the metal surface and to determine the thermodynamic parameters. Every model has its own mathematical representations and allows graphical determination of the necessary parameters [11]. In our study, we evaluated the applicability of all the above models to the adsorption of PDLAE on the carbon steel surface in accordance with their following mathematical expressions, where Cinh is the inhibitor concentration (g·dm^{-3}), θ is the degree of surface coverage, and Kads is the equilibrium constant for absorption-desorption processes:

Langmuir adsorption isotherm:

$$\frac{C_{inh}}{\theta} = \frac{1}{K_{ads}} + C_{inh} \quad (6)$$

Temkin adsorption isotherm:

$$\theta = \ln C_{inh} + K_{ads} \quad (7)$$

Freundlich adsorption isotherm:

$$\log\theta = \log K_{ads} + \frac{1}{n}\log C_{inh} \quad (8)$$

Where n is a dimensionless constant indicating the intensity of the adsorption process. Flory-Huggins adsorption isotherm:

$$\log\frac{\theta}{C_{inh}} = b\log(1-\theta) + \log K_{ads} \quad (9)$$

Where b is the parameter representing the interaction between the adsorbate and the adsorbent. Frumkin Adsorption isotherm:

$$\log\left[C_{inh}\left(\frac{\theta}{1-\theta}\right)\right] = 2a\theta + 2.303\log K_{ads} \quad (10)$$

Where α is the interaction parameter that quantifies the interactions between adsorbed molecules on the surface. El-Awady adsorption isotherm:

$$\log\left(\frac{\theta}{1-\theta}\right) = y\log C_{inh} + \log K \quad (11)$$

$$K_{ads} = K^{\frac{1}{y}}$$

Where y - parameter represents the number of active sites occupied by one molecule of the inhibitor on the metal surface.

The values of the K_{ads} obtained from the isotherms were used to calculate the Gibbs free energy according to the known relationship:

J. of Science and Technology Vol. 17 No. 2 (2025) p. 64-83

$$\Delta G^0_{ads} = -RT \ln(5.55K_{ads}) \quad (12)$$

Where ΔG^0_{ads} is the Gibbs free energy of absorption, R is the universal gas constant (8.314 $J{\cdot}K^{-1}{\cdot}mol^{-1}$), T is the system's thermodynamic temperature, and 55.5 is the molar concentration of water ($mol{\cdot}dm^{-3}$).

The heat of absorption (Q_{ads}) of the inhibitor on the metal surface was obtained for the trend of surface coverage with temperature using the following equation:

$$Q_{ads} = 2.303R \left(\log\frac{\theta_2}{1-\theta_2} - \log\frac{\theta_1}{1-\theta_1}\right) \cdot \left(\frac{T_1 \cdot T_2}{T_2 - T_1}\right) \quad (13)$$

2.5 Electrochemical Measurement

The same pretreatment was applied to the alloy specimens for the electrochemical experiment as for the weight loss test. The Autolab PGSTAT 101 Metrohm potentiostat/galvanostat, equipped with the NOVA 2.1.6 software, was used for the electrochemical test. A three-electrode setup was used for electrochemical measurements: reference electrode (Ag/AgCl filled with 3.0 $mol{\cdot}dm^{-3}$ KCl), counter electrode (platinum), and working electrode (carbon specimen). A beaker containing 100 ml of 1M HCl, both with and without inhibitor, served as the electrochemical cell. The working electrode, with an exposed area of 1.00 cm^2, was stabilized during open circuit potential (OCP) testing. The linear sweep voltammetry (LSV) staircase and corrosion rate analysis were used to perform linear polarization measurements immediately after the OCP. Potentiodynamic scanning was performed with a scan rate of 0.01 $V{\cdot}s^{-1}$ between -0.50 and +0.50 V. From the Tafel polarization curves, the corrosion potential (E_{corr}) and corrosion current density (j_{corr}) were established.

Equation 14 was used to obtain the inhibition efficiency (IE_i%) through the corrosion current density [12]:

$$IE_i(\%) = \frac{i_{inh} - i_{corr}}{i_{inh}} \cdot 100 \quad (14)$$

Where i_{inh} and i_{corr} are the corrosion current densities determined by extrapolating the Tafel slopes with and without inhibitors, respectively, in $A{\cdot}cm^{-2}$.

Using the equation (15), the inhibition efficiency through the polarization resistance (IE_R%) was determined [13]:

$$IE_R(\%) = \frac{R_p^{inh} - R_p^0}{R_p^{inh}} \cdot 100 \quad (15)$$

where R_p^{inh} and R_p^0 represent the charge transfer resistance with and without an inhibitor, respectively, in Ω.

2.6 Contact Angle Measurement

Hydrophilicity of the alloy coupons was assessed by measuring the contact angle between a water drop and the alloy surface using the Ossila Contact Angle Goniometer equipped with the Ossila Contact Angle software *ver.* 4.2.0. The drops of water were mounted on the surface of the metal sample using a micro-syringe with a needle diameter of 0.4 mm. The reported contact angles were an average of at least three measurements on different areas of the surface. Photos of water drops were obtained using a high-resolution video camera and the above software.

3. Results and Discussion

3.1 Weight Loss Assay

At the first step of our research, the inhibition efficiency of PDLAE was evaluated at various inhibitor concentrations (0.1 - 2.0 $g{\cdot}dm^{-3}$), an exposure time of 2 to 24 hours at different temperatures (298-333 K) using a weight loss assay in a 1M HCl solution. The results are shown in Figure 2.

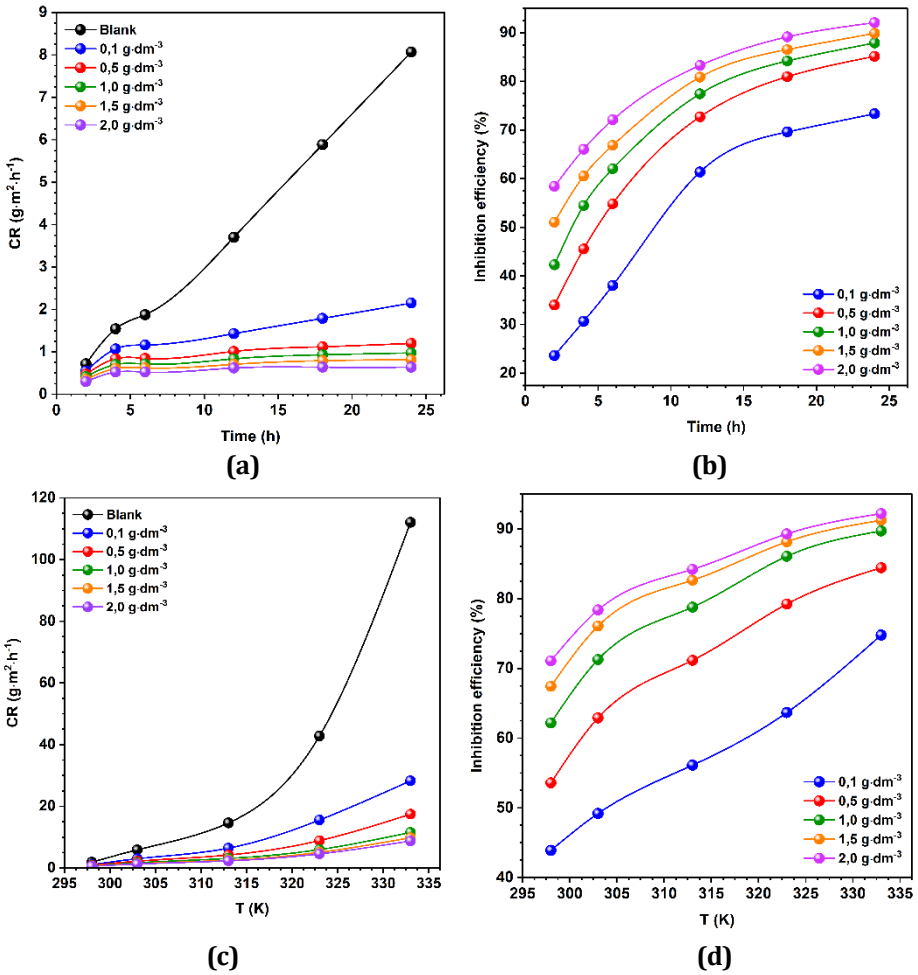

Fig. 2 *Relationship between the corrosion rate (CR) and inhibition efficiency (IE) for PDLAE on carbon steel in 1 M HCl solution at different inhibitor concentrations: (a, b) Immersion time; (c, d) Temperature*

As can be seen in the presence of PDLAE, the CR significantly decreases, particularly at higher inhibitor concentrations (≥1.0 g·dm^{-3}). At 2.0 g·dm^{-3}, the CR remains nearly constant over time, indicating strong inhibition. The lowest concentration (0.1 g·dm^{-3}) shows a less pronounced effect, suggesting that a higher inhibitor concentration is needed for effective corrosion protection. The IE increases with time for all concentrations, eventually stabilizing. At 2.0 g·dm^{-3}, the efficiency reaches 92.07% after 24 hours. The lowest concentration (0.1 g·dm^{-3}) shows a more gradual increase, peaking at 73.34% IE after 24 hours. The trend suggests better adsorption and protective layer formation over time, which enhances the inhibition performance. Despite the increase in temperature, IE remains significant across all concentrations. At 2.0 g·dm^{-3}, the efficiency remains above 80% even at 333 K, demonstrating thermally stable adsorption. The trend suggests that the adsorption of PDLAE follows a physicochemical adsorption mechanism, influenced by temperature but still providing effective corrosion protection.

Corrosion parameters obtained from weight loss assay for carbon steel in 1M HCl solution containing various concentrations of PDLAE at different temperatures at 6 hours of immersion are given in Table 1.

J. of Science and Technology Vol. 17 No. 2 (2025) p. 64-83

Table 1 *Corrosion parameters obtained from weight loss assay for carbon steel in 1M HCl solution containing various concentrations of* PDLAE *at different temperatures at 6 hours of immersion*

Inhibitor concentration, g·dm^{-3}	CR, g·m^{-2}·h^{-1}	IE$_{wl}$%	θ
	298 K		
Blank	1.87	-	-
0.1	1.05	43.90	0.4390
0.5	0.87	53.60	0.5360
1.0	0.71	62.18	0.6218
1.5	0.61	67.43	0.6743
2.0	0.54	71.09	0.7109
	303 K		
Blank	5.88	-	-
0.1	2.99	49.18	0.4918
0.5	2.18	62.89	0.6289
1.0	1.69	71.26	0.7126
1.5	1.41	76.06	0.7606
2.0	1.27	78.37	0.7837
	313 K		
Blank	14.60	-	-
0.1	6.41	56.11	0.5611
0.5	4.21	71.14	0.7114
1.0	3.10	78.79	0.7879
1.5	2.53	82.65	0.8265
2.0	2.31	84.21	0.8421
	323 K		
Blank	42.81	-	-
0.1	15:55	63.67	0.6367
0.5	8.89	79.23	0.7923
1.0	5.96	86.08	0.8608
1.5	5.07	88.16	0.8816
2.0	4.58	89.30	0.8930
	333 K		
Blank	112.07	-	-
0.1	28.26	74.78	0.7478
0.5	17.44	84.44	0.8444
1.0	11.53	89.71	0.8971
1.5	9.81	91.25	0.9125
2.0	8.73	92.21	0.9221

Table 1 shows that the best protective efficiency of 92.21% is achieved at the highest temperature and concentration values. The obtained values of CR and IE clearly indicate an increase in the inhibitory effectiveness of PDLAE with an increase in temperature and concentration in a given corrosion medium. At all temperatures, the IE$_{wl}$ reaches its maximum value at the highest concentration of the inhibitor. The results show that the presence of PDLAE reduces the metal degradation in a 1M HCl solution.

3.2 Activation Parameters Calculations

The graphical representation of activation parameters obtained from the Arrhenius equation and the transition state plots are shown in Figure 3.

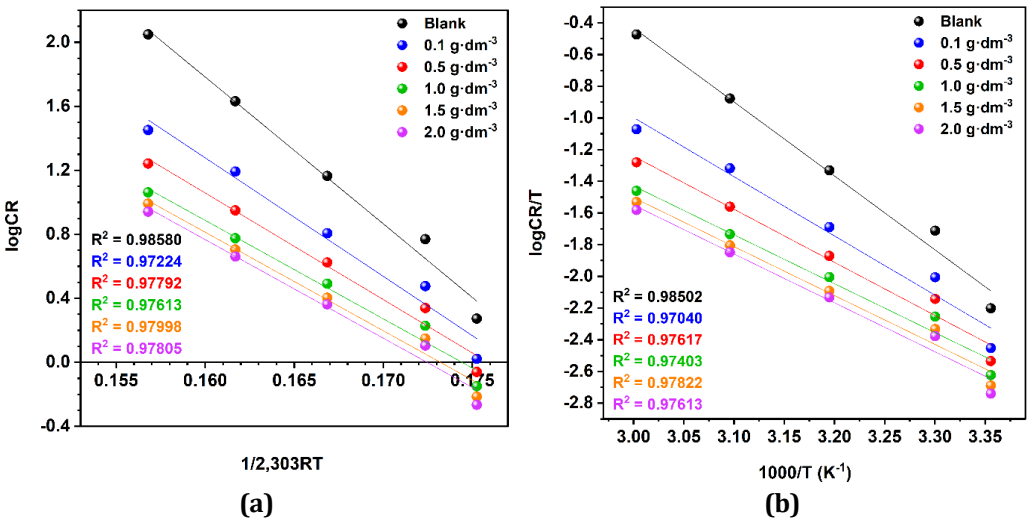

Fig. 3 *Arrhenius and transition state plots for carbon steel in 1M HCl solution in the absence and presence of PDLAE at different concentrations after 4 hours of immersion: (a) Arrhenius plots; (b) Transition state plots*

Table 2 provides insights into the activation parameters of carbon steel dissolution in a 1M HCl solution, both in the absence and presence of different concentrations of PDLAE. The evaluated parameters include the The Arrhenius pre-exponential factor (log A), activation energy (E_a), enthalpy of activation (ΔH*), entropy of activation (ΔS*), and the difference between E_a and ΔH* are given in Table 2.

Table 2 *Activation parameters of the dissolution of carbon steel in 1M HCl solution in the absence and presence of the different concentrations of PDLAE*

Inhibitor concentration, g·dm^{-3}	logA	E_a, kJ·mol^{-1}	ΔH*, kJ·mol^{-1}	ΔS*, J·mol^{-1}·K^{-1}	E_a -ΔH*, kJ·mol^{-1}
Blank	16.46	91.76	89.30	62.04	2.46
0.1	13.12	74.03	71.54	-2.05	2.48
0.5	11.72	66.61	64.11	-29.03	2.50
1.0	10.73	61.51	58.99	-47.97	2.51
1.5	10.66	61.56	59.04	-49.24	2.51
2.0	10.61	61.56	59.05	-50.11	2.51

The activation energy (E_a) for carbon steel dissolution in the uninhibited 1M HCl solution is 91.76 kJ·mol^{-1}, which significantly decreases upon the addition of PDLAE, reaching a minimum value of 61.56 kJ·mol^{-1} at an inhibitor concentration of 2.0 g·dm^{-3}. The values of E_a < 80 kJ·mol^{-1} indicate that the adsorption has a physical nature (physisorption) [14]. A similar trend is observed for log A, where the blank solution has the highest value (16.46), while the lowest value (10.61) is obtained at 2.0 g·dm^{-3}. A decrease in E_a and log A suggests that the inhibitor facilitates the formation of a protective film on the steel surface due to the effective adsorption of the extract components onto the steel surface, reducing the energy barrier required for the corrosion process.

The positive values of the enthalpy of activation (ΔH*) indicate that the corrosion process is endothermic. This implies that the reaction tends to happen spontaneously at higher temperatures and is energetically beneficial. The highest ΔH* value is observed for the blank solution (89.30 kJ·mol^{-1}), while the lowest values (59.04–59.05 kJ·mol^{-1}) correspond to higher inhibitor concentrations (1.5–2.0 g·dm^{-3}). The decrease in ΔH* in the presence of the extract suggests that the corrosion process requires less energy, further confirming the formation of a protective barrier that reduces direct metal dissolution into the acidic medium.

The entropy change (ΔS*), which indicates the disorder at the metal-solution interface during the corrosion process, shifts from 62.04 J·mol^{-1}·K^{-1} (blank) to significantly lower values (-50.11 J·mol^{-1}·K^{-1}) with the highest inhibitor concentration (2.0 g·dm^{-3}). The negative entropy values suggest a more ordered system at the metal-solution interface in the presence of the inhibitor, likely due to the structured adsorption of organic molecules from the extract onto the metal surface [15]. Thus, it indicates the transition state of the corrosion process is more ordered than the initial state. Additionally, it also indicates that the activated complex in the transition state is formed by an association process.

J. of Science and Technology Vol. 17 No. 2 (2025) p. 64-83

Furthermore, the data obtained indicate that the E_a values are more significant than the ΔH* values. The difference E_a - ΔH* remains relatively constant and ranges from 2.46 to 2.51 kJ·mol^{-1}, which is close to the expected value of RT at room conditions (2.61 kJ·mol^{-1}). This consistency supports the validity of the experimental data and suggests that the inhibitive mechanism remains stable across different extract concentrations. This finding suggests that a gas production reaction was a significant part of the corrosion process [15]. However, a slight difference in the theoretical and experimental values of RT may indicate some influence of side reactions and differences in the mechanisms of the corrosion process.

Figure 4 shows the relationship between activation energy (E_a), enthalpy of activation (ΔH*), and log A for carbon steel in 1M HCl solution in the absence and presence of different concentrations of PDLAE.

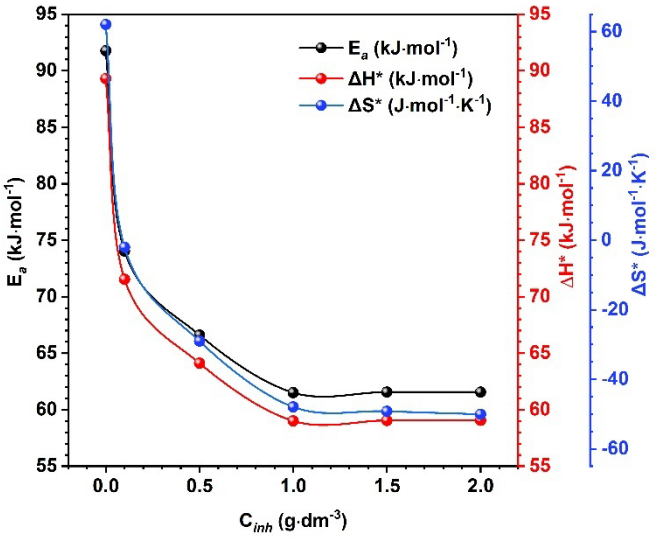

Fig. 4 *The relationship between activation energy (E_a), enthalpy of activation (ΔH*) and log A for carbon steel in 1M HCl solution in absence and the presence of different concentrations of PDLAE*

The obtained activation parameters indicate that the PDLAE effectively inhibits the corrosion of carbon steel in a 1M HCl solution by reducing the activation energy, enthalpy, and entropy of the dissolution process. The decreasing trend suggests that the extract forms a stable protective film on the metal surface, leading to a more controlled and ordered corrosion process. The observed changes in ΔS* further support the strong interaction between inhibitor molecules and the steel surface, reinforcing the inhibition efficiency.

3.3 Absorption and Thermodynamics

In corrosion inhibition studies, adsorption isotherms are fundamental tools for understanding the interaction between inhibitor molecules and the metal surface. Isotherms are mathematical models used in corrosion studies to describe the adsorption behavior of inhibitors on metal surfaces. They provide insights into the interaction mechanisms between the inhibitor molecules and the metal, which is critical for understanding and optimizing corrosion protection. Commonly used adsorption isotherms in corrosion studies include Langmuir, Freundlich, Temkin, Frumkin, Florry-Huggins, and El-Awady isotherms, each describing different interaction mechanisms between inhibitors and metal surfaces. In this work, we applied all these models to estimate the adsorption mechanism of PDLAE on the carbon steel surface.

Figure 5 shows the adsorption isotherms of PDLAE on the carbon steel surface in a 1M HCl solution at all experimental temperatures.

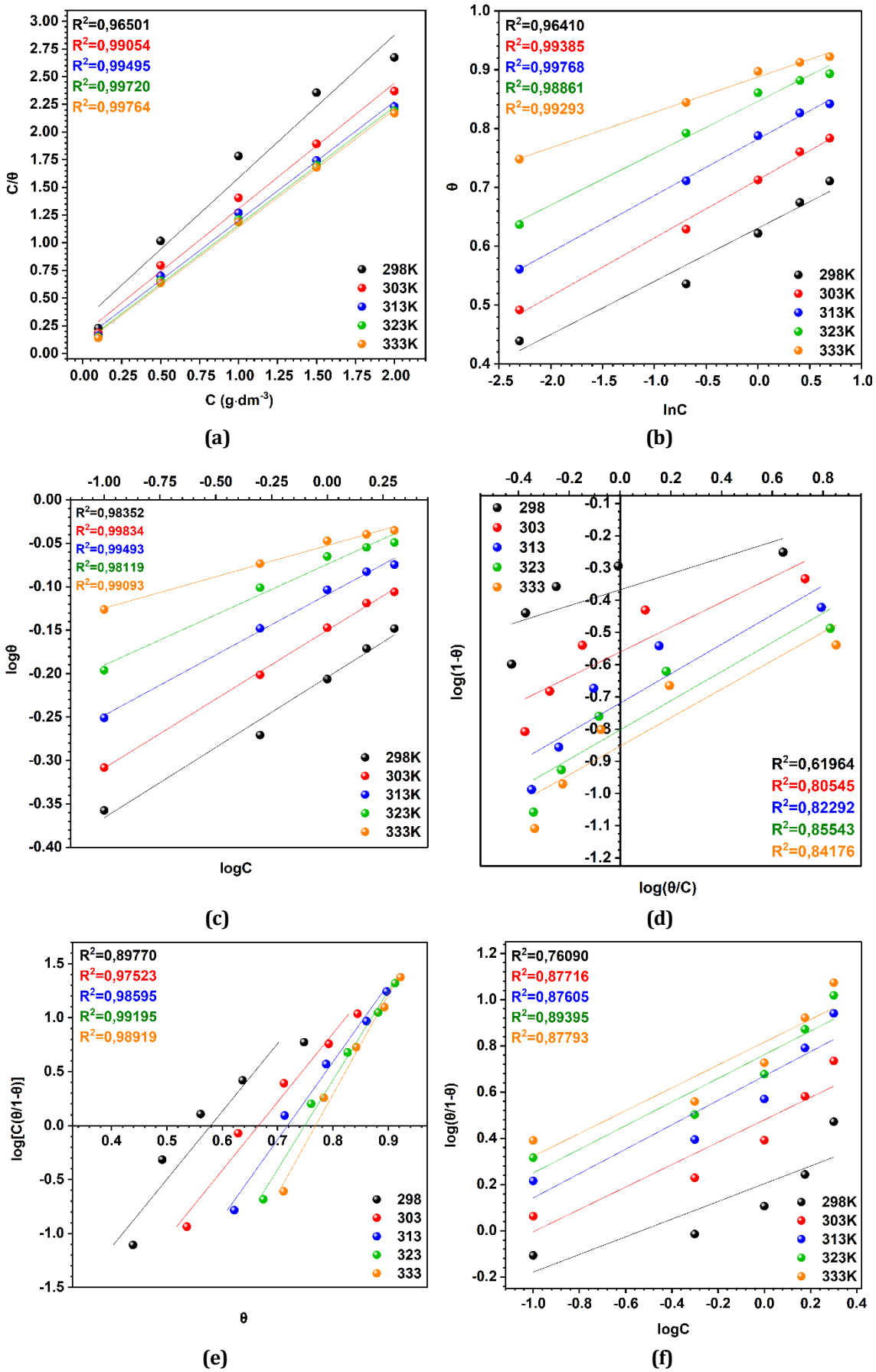

Fig. 5 *Adsorption isotherms for PDLAE on the carbon steel surface in 1M HCl solution for a 4-hour immersion period: (a) Langmuir; (b) Temkin; (c) Freundlich; (d) Flory-Huggins; (e) Frumkin; (f) El-Awady*

J. of Science and Technology Vol. 17 No. 2 (2025) p. 64-83

Figure 5 shows that plots of C/θ *vs* C are presented as a straight line at all experimental temperatures. The linear approximation with correlation coefficient values (R^2) more than 0.99 indicates that the Langmuir model is the most suitable for describing the PDLAE adsorption mechanism on the carbon steel surface. The obeying of the adsorption with the Langmuir model confirms that the inhibitor molecules form a monolayer on the carbon steel surface, meaning that each active site on the metal surface is occupied by only one inhibitor molecule without multilayer formation. This implies that the metal surface is homogeneous, with all adsorption sites being energetically equivalent. Furthermore, the Langmuir model assumes no lateral interactions between the adsorbed molecules, indicating that the adsorption of one molecule does not significantly influence the adsorption of another. In addition, this indicates that the water molecules on the metal surface are displaced by the inhibitor molecules as a result of absorption from the solution, forming the protective layer of the inhibitor [16].

The slopes and intercepts of the plots were used to calculate the K_{ads} and Gibbs free energy (ΔG^0_{ads}) values for the PDLAE. The obtained thermodynamic parameters are shown in Table 3.

Table 3 *Thermodynamic parameters of adsorption of PDLAE on carbon steel surface in 1M HCl solution obtained from adsorption isotherms*

Isotherm	T, K	Slope	Intercept	R^2	K_{ads}	ΔG^0_{ads}, kJ·mol^{-1}	Isotherm property
	298	1.29023	0.29534	0.96501	3.39	-12.97	-
	303	1.13378	0.17335	0.99054	5.77	-14.54	-
Langmuir	313	1.07586	0.12337	0.99495	8.11	-15.90	-
	323	1.06685	0.09361	0.99720	10.68	-17.15	-
	333	1.06020	0.08157	0.99764	12.26	-18.06	-
	298	0.09029	0.63965	0.96410	0.64	-8.85	-
	303	0.09896	0.71310	0.99385	0.71	-9.27	-
Temkin	313	0.09611	0.78226	0.99768	0.78	-9.81	-
	323	0.08818	0.84633	0.98861	0.85	-10.34	-
	333	0.06001	0.88755	0.99293	0.89	-10.79	-
							n
	298	0.16181	-0.20415	0.98352	0.62	-8.79	6.18
	303	0.15866	-0.15013	0.99834	0.71	-9.25	6.30
Freundlich	313	0.13906	-0.10904	0.99493	0.78	-9.80	7.19
	323	0.11634	-0.07406	0.98119	0.84	-10.33	8.60
	333	0.07215	-0.05247	0.99093	0.89	-10.79	13.86
							b
	298	0.24762	-0.36759	0.61964	0.43	-7.86	0.25
	303	0.38687	-0.56111	0.80545	0.27	-6.86	0.39
Flory-Huggins	313	0.45609	-0.71945	0.82292	0.19	-6.14	0.46
	323	0.45372	-0.80301	0.85543	0.16	-5.82	0.45
	333	0.44254	-0.85327	0.84176	0.14	-5.68	0.44
							α
	298	0.15897	0.57918	0.89770	1.78	-11.39	0.08
	303	0.15775	0.66551	0.97523	1.95	-11.80	0.08
Frumkin	313	0.13865	0.71814	0.98595	2.05	-12.32	0.07
	323	0.12089	0.74915	0.99195	2.11	-12.80	0.06
	333	0.10835	0.76865	0.98919	2.16	-13.25	0.05
							1/y
	298	0.38226	0.20334	0.76090	8.36	-15.21	5.23
	303	0.48439	0.47973	0.87716	12.46	-16.48	4.13
El-Awady	313	0.52721	0.66925	0.87605	17.71	-17.93	3.79
	323	0.51154	0.76148	0.89395	22.58	-19.16	3.91
	333	0.49356	0.81563	0.87793	26.50	-20.20	4.05

Negative values of ΔG^0_{ads} indicate the spontaneity of the adsorption process of the PDLAE on the carbon steel surface [17]. It is evident from the value of $\Delta G^0_{ads} > -20$ kJ·mol^{-1} that the adsorption is physical (physisorption) and results from an electrostatic interaction between the alloy surface and charged inhibitor molecules [18]. In this case, the process is driven by weak van der Waals forces, dipole interactions, and hydrogen bonding, and the inhibitor molecules are loosely attached to the metal surface, making adsorption reversible and temperature-dependent. Increasing temperature and the inhibitor concentration accelerates the adsorption-desorption processes, leading to the formation of a stable protective barrier on the metal surface [19].

The values of ΔH^0_{ads} and ΔS^0_{ads} were revealed from the obtained values of ΔG^0_{ads} using the rearranged Gibbs-Helmholtz equation as follows:

$$\Delta G^0_{ads} = \Delta H^0_{ads} - T\Delta S^0_{ads} \quad (16)$$

The slope and intercept of the plot of the relationship between ΔG0ads and T allow to determine the values of ΔG^0_{ads} using the rearranged Gibbs-Helmholtz equation as follows:

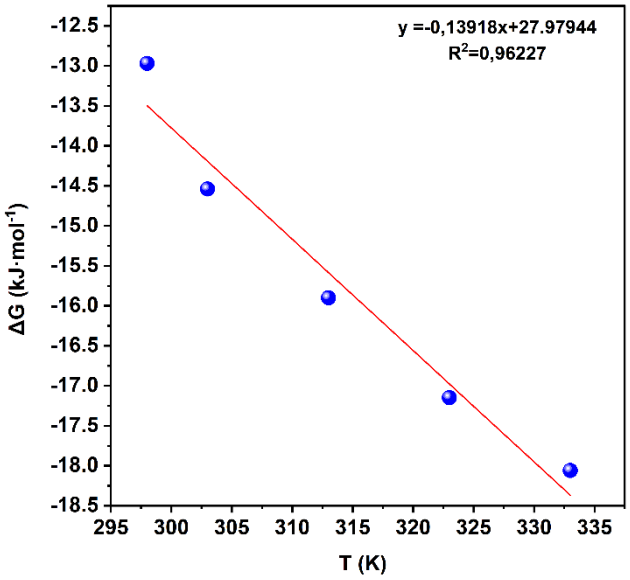

Fig. 6 *The relationship between Gibbs free energy (ΔG^0_{ads}) and absolute temperature (T) for carbon steel in 1M HCl*

The positive value of ΔH^0_{ads} (27.98 kJ·mol^{-1}) shows that the adsorption of the inhibitor on the carbon steel surface is an endothermic process, which means that higher temperatures favor adsorption, which is consistent with the decreasing trend of ΔG^0_{ads} at elevated temperatures. Endothermic adsorption implies an interaction between the inhibitor molecules and the metal surface leading to physisorption. In addition, this suggests that the adsorption process accelerates with increasing temperature since higher thermal energy makes it easier to overcome the activation barrier of the adsorption [20].

The positive ΔS^0_{ads} value (139.18 J·mol^{-1}·K^{-1}) indicates that the adsorption process is accompanied by an increase in system disorder due to the desorption of pre-adsorbed water molecules from the metal surface. These results are attributed to endothermic adsorption (positive ΔH^0_{ads}) and suggest that adsorption is entropy-driven, which is typical for systems where organic molecules replace water molecules on the metal surface [21].

The results confirm that the inhibitor adsorption on the carbon steel surface in 1M HCl is spontaneous and becomes stronger with increasing temperature. The observed trend suggests a mixed adsorption mechanism involving both physical and chemical interactions, where the inhibitor molecules form a protective layer that enhances corrosion resistance at higher temperatures.

Table 4 displays the results of the heat of adsorption (Q_{ads}, kJ·mol^{-1}) calculations made using Equation 13.

Table 4 *Adsorption heat (Q_{ads}, kJ·mol^{-1}) values for PDLAE on carbon steel surface in 1M HCl solution at different temperature ranges*

Temperature range, K	T_2-T_1, K	Inhibitor concentration, g·dm^{-3}				
		0.1	0.5	1.0	1.5	2.0
298-303	5	31.93	57.58	61.72	64.30	58.24
303-313	10	21.95	29.55	31.85	31.91	30.48
313-323	10	26.52	36.72	42.83	37.56	37.64
323-333	10	47.05	31.50	30.77	30.10	31.27
298-313	15	22.90	33.03	42.84	43.79	40.71
298-323	25	25.44	37.69	41.77	40.37	38.55
298-333	35	31.41	36.48	39.33	38.10	37.05

J. of Science and Technology Vol. 17 No. 2 (2025) p. 64-83

Figure 7 illustrates the variation in the heat of adsorption (Q_{ads}, kJ·mol^{-1}) for PDLAE on a carbon steel surface in 1M HCl solution as a function of temperature and temperature difference.

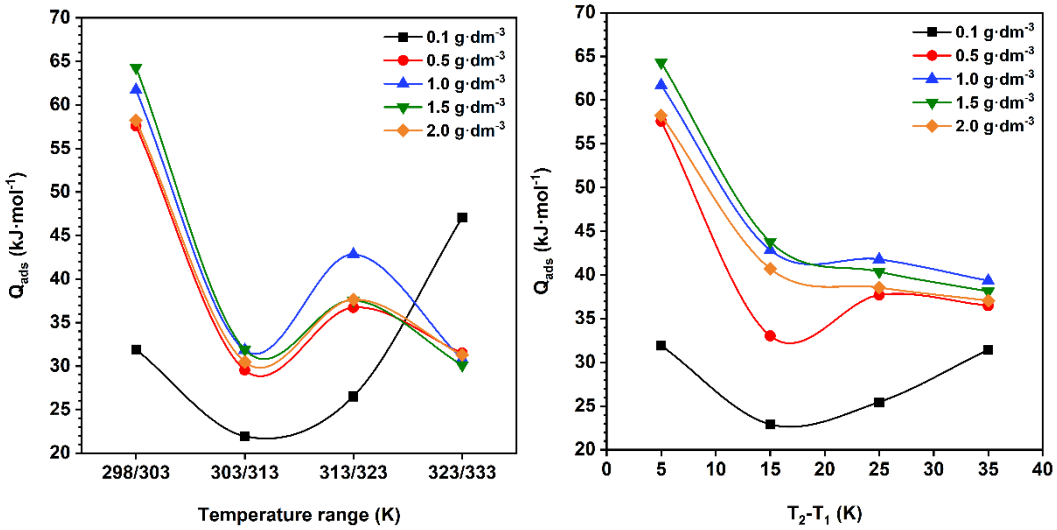

Fig. 7 *Change in the heat of adsorption (Q_{ads}, kJ·mol^{-1}) for PDLAE on carbon steel surface in 1M HCl solution: (a) With increasing in temperature; (b) At different temperature ranges*

As can be seen, in both plots, the adsorption heat exhibits a distinct non-monotonic trend, initially decreasing with increasing temperature, reaching a minimum, and then rising again at higher temperatures. This behavior suggests a temperature-dependent adsorption mechanism, where lower temperatures favor strong initial adsorption, but increased thermal energy at higher temperatures alters molecular interactions. The minimum observed in Q_{ads} values around 303-313 K (Fig. 7A) may indicate a transition between different adsorption mechanisms, possibly shifting from physical to chemical adsorption [22]. The relatively higher values of Q_{ads} at low inhibitor concentrations (0.1 g·dm^{-3}) suggest weaker adsorption interactions, while higher concentrations (≥ 0.5 g·dm^{-3}) exhibit more stable behavior. The decrease in adsorption heat with increasing temperature difference (Fig. 7B) supports the hypothesis that adsorption is predominantly exothermic. The observed changes in Q_{ads} suggest a mixed adsorption mechanism, involving both physisorption and chemisorption, which is a typical characteristic of plant-derived corrosion inhibitors.

3.4 Contact Angle Measurement

Measuring the contact angle on a metal surface in corrosion studies provides crucial insights into the wettability and surface energy of the metal before and after inhibitor adsorption. The contact angle reflects the extent to which a liquid (typically water) spreads on the surface, which is directly related to surface hydrophilicity or hydrophobicity. A high contact angle indicates reduced wettability and increased hydrophobicity, suggesting the formation of a protective inhibitor layer that hinders electrolyte penetration, thereby improving corrosion resistance, and *vice versa*.

Figure 8 shows micrographs of the metal surface and the value of the contact angle before and after immersion of the metal specimen in 1M HCl solution with and without PDLAE.

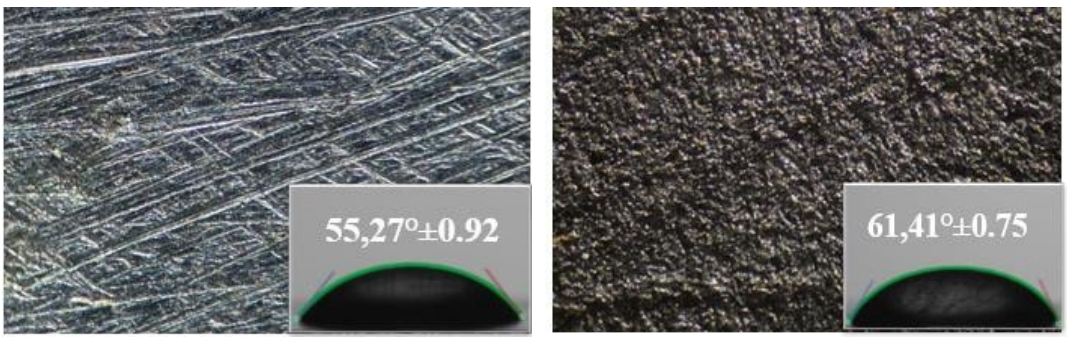

(a) **(b)**

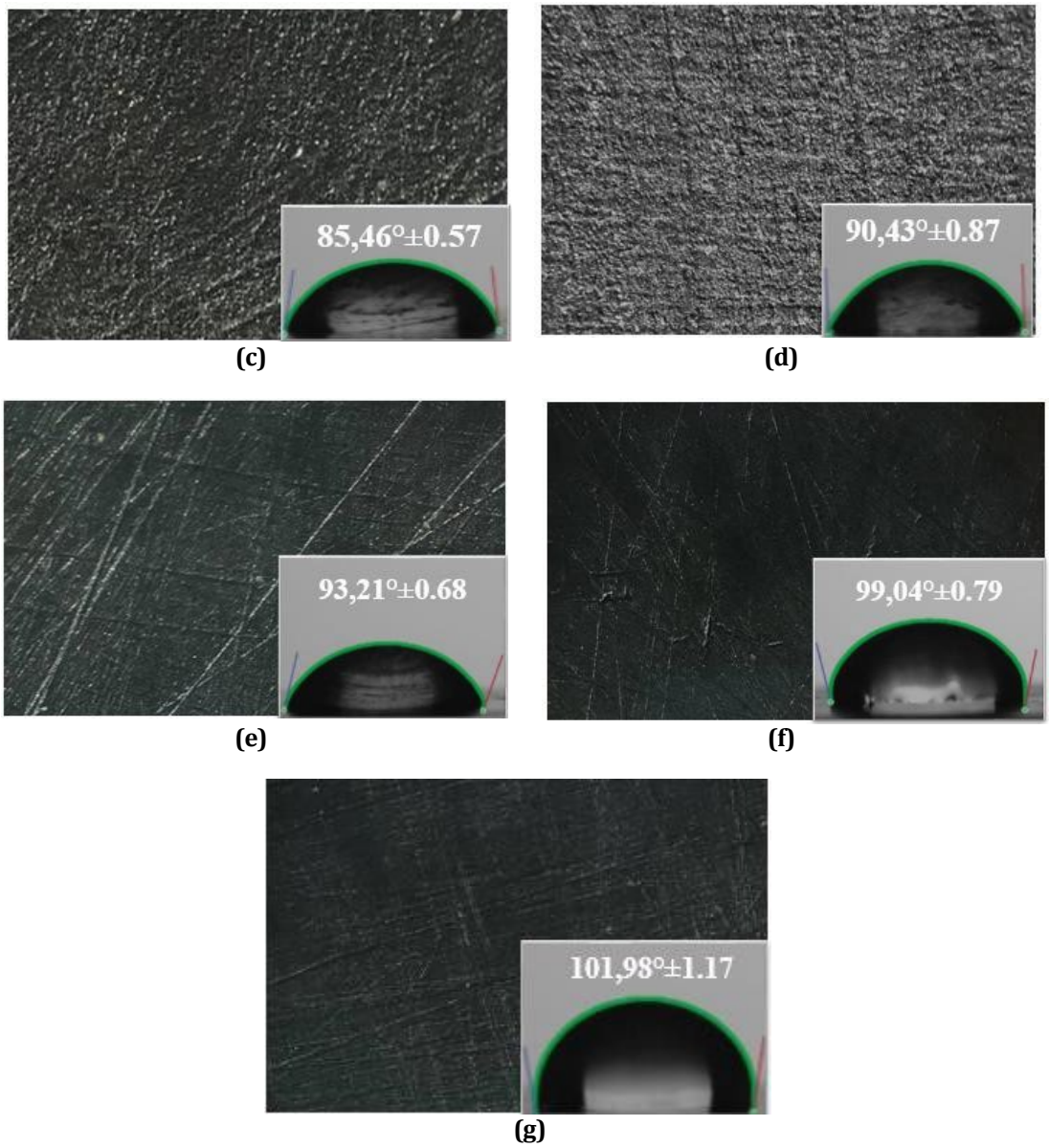

Fig. 8 *Micrographs (x50) and contact angle of the carbon steel surface after 24 h of immersion in a 1M HCl solution with the presence and absence of PDLAE: (a) blank before immersion; (b) blank after immersion; (c) 0.1 g·dm^{-3}; (d)0.5 g·dm^{-3}; (e) 1.0 g·dm^{-3}; (f) 1.5 g·dm^{-3}; (g) 2.0 g·dm^{-3}*

Before immersion in the corrosive medium, the polished carbon steel surface exhibited a contact angle of 52.27° ± 0.92, as illustrated in Figure 8. After 24 hours of exposure to 1M HCl without an inhibitor, the contact angle increased to 61.41° ± 0.75. The presence of the inhibitor led to a significant rise in the contact angle, which increased proportionally with concentration, reaching a maximum of 101.98° ± 1.17 after 24 hours of immersion. The progressive increase in contact angle values indicates enhanced surface hydrophobicity with higher inhibitor concentrations. This indicates that the inhibitor forms a protective layer on the metal surface, reducing its wettability by effectively adsorbing onto it. As the inhibitor concentration increases, this barrier becomes more robust, further limiting the interaction between the corrosive solution and the carbon steel surface.

As can also be observed, before exposure to the corrosive environment, the steel specimen exhibited a uniform surface with a distinct metallic luster, indicative of its intact structure. However, significant structural alterations were observed upon immersion in an acidic solution without the presence of an inhibitor. Dark, porous, and loosely adhered corrosion products were formed, characterized by visible pits and cracks, which suggests extensive metal degradation. These surface defects can accelerate the corrosion process by facilitating further penetration of the aggressive medium. In contrast, in the presence of PDLAE, a protective film formed on the metal surface, reducing direct contact with the corrosive solution. As a result, the metallic sheen diminished,

J. of Science and Technology Vol. 17 No. 2 (2025) p. 64-83

but the underlying metal structure remained largely intact. This confirms that the inhibitor significantly reduces corrosion damage by forming a protective layer that effectively shields the metal from further degradation.

3.5 UV-Visible Spectroscopy Analysis

In corrosion studies, UV spectroscopy is used to establish the adsorption of the inhibitor on the metal surface. This technique helps in determining the concentration of the inhibitors in solution before and after exposure to the metal, which reveals the extent of adsorption. Changes in absorption intensity or peak shift indicate possible chemical or physical adsorption mechanisms. This method is particularly useful for evaluating the efficiency of plant-based inhibitors, as their natural compounds exhibit strong UV absorption due to conjugated double bonds, aromatic rings, or other chromophores. Figure 9 shows the UV spectra of the corrosive medium containing PDLAE before and after 24-hour exposure of the carbon steel specimen.

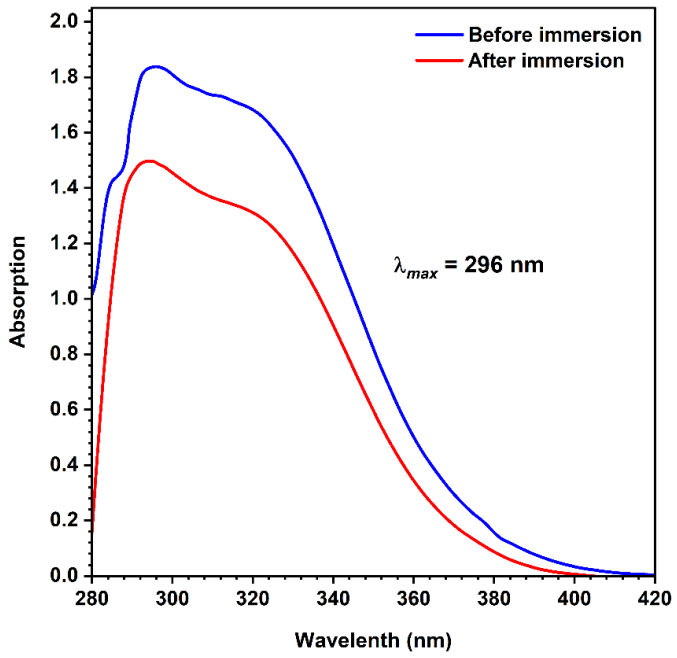

Fig. 9 *UV–vis spectra of 1M HCl solution containing 0.5 g·dm^{-3} of PDLAE before (blue line) and after 24 h of immersion (red line) of carbon*

The UV-Vis spectra of the solution, both before and after immersion, indicate that the highest absorption, characteristic of phenolic phytocomponents, is observed at 296 nm [23]. The absorption in both cases is solely attributed to the constituents of the examined extract. However, a significant decrease in absorption intensity is evident after the metal specimen has been immersed in the corrosive environment for 24 hours in the presence of 0.5 g·dm^{-3} of the inhibitor. Notably, the maximum absorption wavelength remains unchanged, suggesting that the extract's components do not undergo chemical interactions with metal ions or the corrosive medium, which also confirms the physical nature of the adsorption. The observed hypochromic effect is attributed to the adsorption of phytocomponents onto the metal surface, leading to their reduced concentration in the solution.

3.6 Electrochemical Experiment

The electrochemical behavior of carbon steel in 1M HCl solution, both in the absence and presence of different concentrations of PDLAE, is depicted in Figure 10.

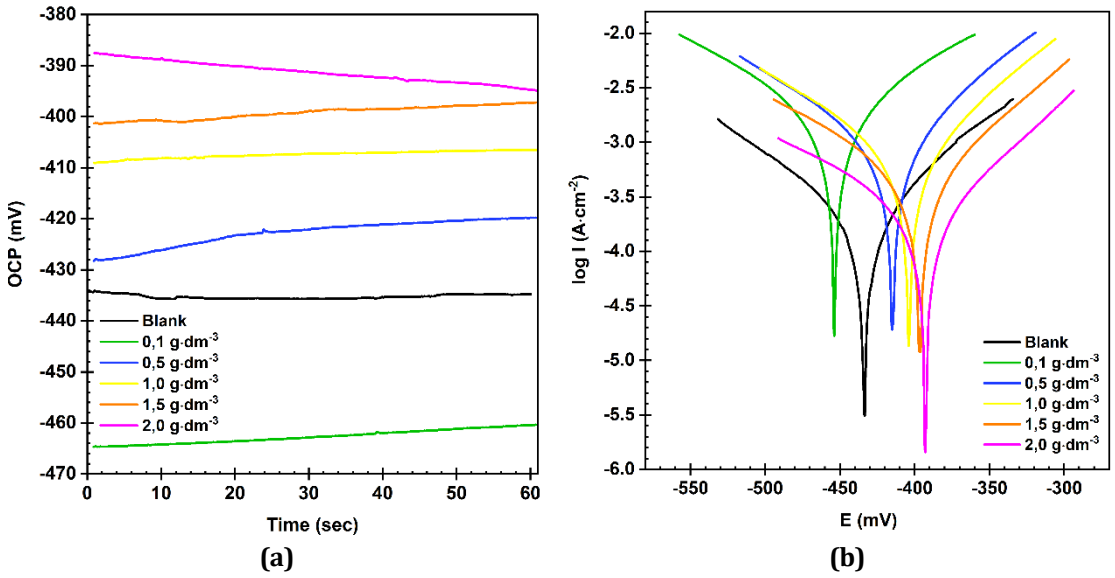

Fig. 10 *OCP vs. time diagram and Tafel polarization curves for carbon steel in 1 M HCl solution with and without PDLAE at room temperature: (a) OCP vs. time; (b) Tafel polarization curves*

The open circuit potential (OCP) *vs.* time diagram (Fig. 10A) demonstrates a gradual shift in potential towards more positive values as the inhibitor concentration increases, indicating the formation of a protective layer on the metal surface. The blank solution exhibits the most negative potential, signifying the highest corrosion susceptibility, whereas the sample with 2.0 g·dm^{-3} of inhibitor shows the most positive potential, suggesting enhanced corrosion resistance. The Tafel polarization curves (Fig. 10B) reveal a significant reduction in corrosion current density (I_{corr}) with increasing inhibitor concentration. The shift in both anodic and cathodic branches suggests that the extract acts as a mixed-type inhibitor, affecting both metal dissolution and hydrogen evolution reactions. The observed decrease in I_{corr} and the shift in corrosion potential (E_{corr}) confirm the inhibitory effect of the extract, highlighting its efficiency in mitigating carbon steel corrosion in acidic media.

Table 5 presents the electrochemical corrosion parameters of carbon steel in 1M HCl in the absence and presence of various concentrations of PDLAE at room temperature.

Table 5 *The electrochemical corrosion parameters of carbon steel in 1M HCl in the absence and presence of different concentrations of PDLAE at room temperature*

Concentration, g·dm^{-3}	-E_{corr}, mV	J_{corr}, A·cm^{-2}	IE_i, %	$\|b_a\|$, mV·dec^{-1}	$\|b_c\|$, mV·dec^{-1}	R_p, Ω	IE_R, %
0.0	453.56	$9.38\cdot10^{-5}$	-	87.58	94.97	142.85	-
0.1	433.65	$5.89\cdot10^{-5}$	37.24	80.77	99.39	239.83	40.44
0.5	414.73	$5.42\cdot10^{-5}$	42.20	96.37	105.10	297.42	51.97
1.0	403.67	$3.94\cdot10^{-5}$	57.98	114.95	107.71	343.92	58.46
1.5	396.50	$2.05\cdot10^{-5}$	78.10	105.58	97.58	480.45	70.27
2.0	380.92	$1.20\cdot10^{-5}$	87.19	87.23	91.92	545.43	73.81

The corrosion potential (E_{corr}) shifts to more positive values upon inhibitor addition, suggesting a reduction in the thermodynamic tendency of the metal to corrode. The anodic ($|b_a|$) and cathodic ($|b_c|$) Tafel slopes exhibit moderate variations, suggesting that the inhibitor influences both metal dissolution and hydrogen evolution reactions, confirming its mixed-type behavior [24]. The charge transfer resistance (R_p) increases significantly with inhibitor concentration, reaching 485.43 Ω at 2.0 g·dm^{-3}, reflecting enhanced surface protection [25]. The inhibition efficiency derived from polarization resistance (IE_R) aligns with that calculated from J_{corr}, further validating the effectiveness of PDLAE in the protection of carbon steel corrosion in acidic environments.

These findings highlight the high potential of PDLAE as a sustainable green corrosion inhibitor for carbon steel in acidic environments, aligning with green chemistry principles.

3.7 Fourier-Transform Infrared Spectroscopy (FTIR) Analysis

Infrared (IR) spectroscopy, particularly FTIR, is widely used in the study of plant-based corrosion inhibitors. Analyzing IR spectra of plant extracts enables to identify the functional groups and bioactive compounds

J. of Science and Technology Vol. 17 No. 2 (2025) p. 64-83

responsible for corrosion inhibition, understand their interaction with metal surfaces, and validate the extract's effectiveness as a natural, eco-friendly inhibitor. The FTIR spectrum of PDLAE is shown in Fig. 11.

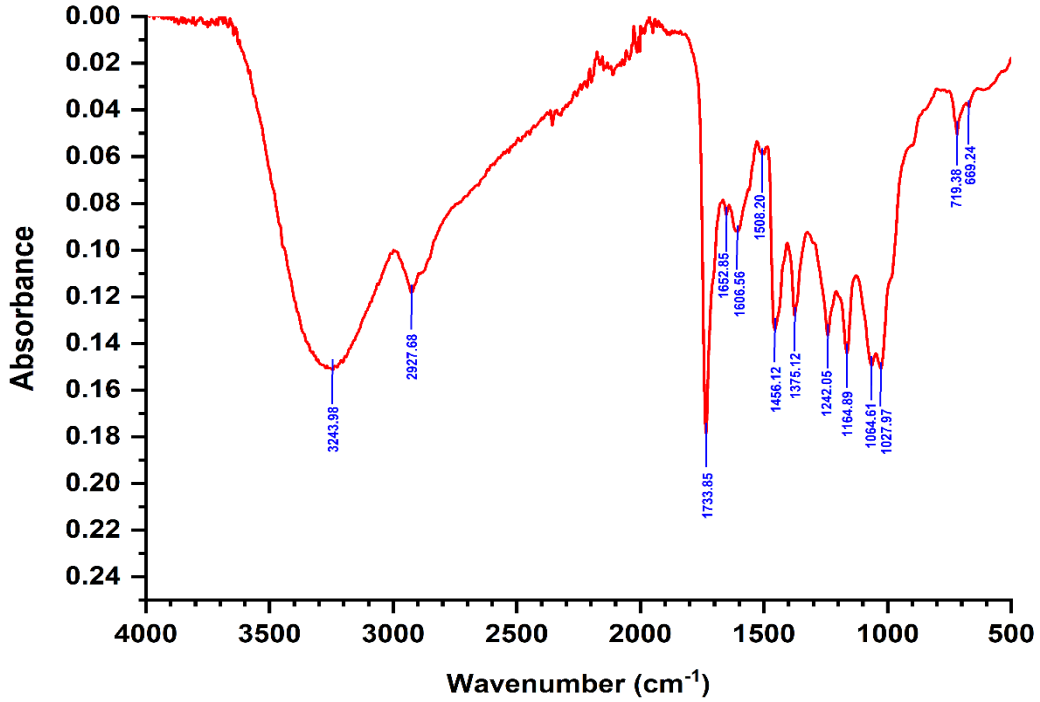

Fig. 11 FTIR spectrum of PDLAE

Table 6 displays the correspondence of the absorption bands and the potential nature of the phytocomponents of the PDLAE.

Table 6 *FTIR absorption bands and corresponding functional groups in PDLAE*

Wavenumber (cm^{-1})	Functional Group	Assignment	Probable phytocomponents
3243.98	–OH (Hydroxyl)	O–H stretching (H-bonded)	Polyphenols, flavonoids, tannins
2927.68	$–CH_2$ / $–CH_3$	Aliphatic C–H stretching	Lipids, terpenoids
1733.85	C=O	Carbonyl stretching (ester/acid)	Flavonoid glycosides, fatty acid esters
1652.85	C=C / C=O (conjugated)	Aromatic C=C / conjugated C=O stretch	Phenolic acids, flavonoids
1606.55	C=C (Aromatic)	Aromatic ring stretching	Flavonoids, lignins
1508.20	Aromatic ring	Skeletal vibration	Phenolics, flavonoids
1455.12	$–CH_2$ / $–CH_3$	Bending vibration	Terpenoids, lipids
1375.12	$–CH_3$	Symmetric deformation	Terpenoids
1242.05	C–O–C / C–O	Ether or ester stretching	Glycosides, phenolics
1164.89	C–O	C–O stretching (alcohol/ester)	Flavonoid glycosides, sugars
1064.61	C–O / C–O–C	Ether/alcohol stretching	Carbohydrates, glycosides
1027.97	C–O	Polysaccharide stretching	Glycosides, polyols
719.38, 669.24	=C–H (Aromatic or alkene)	Out-of-plane bending	Aromatic compounds, phenolics

The FTIR spectrum of the PDLAE revealed characteristic absorption bands corresponding to various functional groups indicative of major phytochemical constituents. A broad and intense band observed at 3243.98 cm^{-1} is attributed to O–H stretching vibrations of hydroxyl groups, which are commonly found in polyphenols, flavonoids, and tannins. The absorption at 2927.68 cm^{-1} corresponds to aliphatic C–H stretching vibrations, typically associated with $–CH_2$ and $–CH_3$ groups, indicating the presence of lipophilic compounds such as terpenoids and fatty acids. A prominent peak at 1733.85 cm^{-1} is assigned to C=O stretching vibrations,

characteristic of ester or carboxylic acid functional groups, suggesting the presence of flavonoid glycosides or esterified phenolic acids. The strong band at 1652.85 cm^{-1} and a nearby peak at 1606.55 cm^{-1} indicate C=C stretching in aromatic systems or conjugated C=O groups, further confirming the presence of phenolic structures such as flavonoids and phenolic acids. A series of peaks in the region from 1508.20 cm^{-1} to 1375.12 cm^{-1} represent skeletal vibrations of aromatic rings and C–H bending modes, commonly associated with flavonoids and lignin derivatives. The absorption bands at 1242.05 cm^{-1}, 1164.89 cm^{-1}, 1064.61 cm^{-1}, and 1027.97 cm^{-1} are characteristic of C–O and C–O–C stretching vibrations, indicating the presence of glycosidic linkages, alcohols, and polysaccharides, which are commonly found in flavonoid glycosides and plant-derived carbohydrates. In addition, weak absorptions at 719.38 cm^{-1} and 669.24 cm^{-1} correspond to out-of-plane bending vibrations of =C–H bonds in aromatic or alkene structures, further supporting the presence of phenolic and aromatic compounds.

In summary, the FTIR analysis confirms that the *P. domestica* leaf extract comprises a complex mixture of phytoconstituents, predominantly flavonoids, phenolics, glycosides, and polysaccharides. The spectrum reveals a high content of polyphenolic compounds, particularly flavonoids and phenolic acids, along with carbohydrate-based constituents such as glycosides. The presence of specific hydroxyl and carbonyl groups, along with ring structures, highlights the active properties of the extract. These features collectively suggest significant antioxidant potential and support its prospective application as a natural, environmentally benign corrosion inhibitor.

4. Conclusion

This study highlights the potential of PDLAE as an eco-friendly and effective corrosion inhibitor for carbon steel in 1M HCl solution. The extract demonstrated remarkable inhibition efficiency, reaching up to 92.07% at optimal concentrations, and maintaining stability across varying temperatures. Thermodynamic analyses revealed that the adsorption process is spontaneous and obeys the Langmuir isotherm model, indicating monolayer formation on the metal surface. Electrochemical measurements confirmed the mixed-type inhibition behavior, effectively reducing both anodic and cathodic reactions. Furthermore, contact angle studies showed enhanced hydrophobicity of the metal surface in the presence of the inhibitor, contributing to improved corrosion resistance. The observed non-monotonic trend of the heat of adsorption (Qads) with temperature suggests a possible transition between physical and chemical adsorption processes. At lower temperatures, physisorption dominates, while higher thermal energy facilitates chemisorption. The positive value of ΔH0ads confirms the endothermic nature of adsorption, indicating enhanced efficiency at elevated temperatures. The findings highlight the importance of plant-based inhibitors in advancing sustainable corrosion protection strategies, aligning with green chemistry principles.

Acknowledgement

The authors gratefully acknowledge the head and staff of the Laboratory of Ecology and Biogeochemistry of M. Utemisov West Kazakhstan University for providing the necessary facilities, technical support, and assistance to conduct this research.

Conflict of Interest

The authors declare that there is no conflict of interest regarding the publication of the paper.

Author Contribution

The authors confirm contribution to the paper as follows: ***study conception and design:*** *Nikolay Akatyev, Meryuet Khapiyeva;* ***data collection:*** *Meryuet Khapiyeva, Roza Kenzhegalieva, Aruzhan Talapova, Gaukhar Uzakbay, Aikorkem Tlektes, Alexandra Logashkina;* ***analysis and interpretation of results:*** *Meryuet Khapiyeva, Roza Kenzhegalieva, Aruzhan Talapova, Gaukhar Uzakbay;* ***draft manuscript preparation:*** *Meryuet Khapiyeva, Roza Kenzhegalieva, Aruzhan Talapova, Gaukhar Uzakbay. All authors reviewed the results and approved the final version of the manuscript.*

References

[1] Nnanna, L., Nnanna, G., Nnakaife, J., Ekekwe, N., & Eti, P. (2016). Aqueous extracts of *Pentaclethra macrophylla bentham* roots as eco-friendly corrosion inhibition for mild steel in 0.5 M KOH medium. *International Journal of Materials and Chemistry*, *6*(1), 12-18, https://doi.org/10.5923/j.ijmc.20160601.03

[2] Liu, W., Nan, G., Nisar, M. F., & Wan, C. (2020). Chemical constituents and health benefits of four Chinese plum species. *Journal of Food Quality*, *2020*(1), 8842506, https://doi.org/10.1155/2020/8842506

[3] El-Beltagi, H. S., El-Ansary, A. E., Mostafa, M. A., Kamel, T. A., & Safwat, G. (2019). Evaluation of the phytochemical, antioxidant, antibacterial, and anticancer activity of *Prunus domestica* fruit. *Notulae Botanicae Horti Agrobotanici Cluj-Napoca*, *47*(2), 395-404, https://doi.org/10.15835/nbha47111402

[4] Stierlin, E., Azoulay, S., Massi, L., Fernandez, X., & Michel, T. (2018). Cosmetic potentials of *Prunus domestica L.* leaves. *Journal of the Science of Food and Agriculture*, *98*(2), 726-736, https://doi.org/10.1002/jsfa.8520

[5] Makovics-Zsohár, N., Tóth, M., Surányi, D., Kovács, S., Hegedűs, A., & Halász, J. (2017). Simple sequence repeat markers reveal Hungarian plum (*Prunus domestica L.*) germplasm as a valuable gene resource. *HortScience*, *52*(12), 1655-1660, https://doi.org/10.21273/HORTSCI12406-17

[6] Abd-El-Nabey, B. A., Mohamed, M. E., Helmy, A. M., Elnagar, H., & Abdel-Gaber, A. M. (2024). Eco-friendly corrosion inhibition of steel in acid pickling using *Prunus domestica* seeds and Okra stems extracts. *International Journal of Electrochemical Science*, *19*(8), 100695, https://doi.org/10.1016/j.ijoes.2024.100695

[7] Kamran, M., Shah, A. U. H. A., Rahman, G., & Bilal, S. (2022). Potential impacts of *Prunus domestica* based natural gum on physicochemical properties of polyaniline for corrosion inhibition of mild and stainless steel. *Polymers*, *14*(15), 3116, https://doi.org/10.3390/polym14153116

[8] Sanni, O., Ren, J., & Jen, T. C. (2022, October). Exploring the Potential Role of *Prunus domestica* in Corrosion Inhibition of AA6063-T5 Aluminium Alloy in Sodium Chloride Media. In *ASME International Mechanical Engineering Congress and Exposition* (Vol. 86656, p. V003T03A030). American Society of Mechanical Engineers, https://doi.org/10.1115/IMECE2022-94911

[9] ISO 8407-2021 Corrosion of metals and alloys—Removal of corrosion products from corrosion test specimens (2021). Geneva, Switzerland

[10] Hamdy, A., & El-Gendy, N. S. (2013). Thermodynamic, adsorption, and electrochemical studies for corrosion inhibition of carbon steel by henna extract in acid medium. *Egyptian Journal of Petroleum*, 22(1), 17–25, https://doi.org/10.1016/j.ejpe.2012.06.002

[11] Popoola, L. T. (2019). Organic green corrosion inhibitors (OGCIs): a critical review. *Corrosion Reviews*, *37*(2), 71-102, https://doi.org/10.1515/corrrev-2018-0058

[12] Li, B., Wang, W., Chen, L., Zheng, X., Gong, M., Fan, J., ... & Zhu, G. (2023). Corrosion inhibition effect of *Magnolia grandiflora* leaves extract on mild steel in acid solution. *International Journal of Electrochemical Science*, *18*(4), 100082, https://doi.org/10.1016/j.ijoes.2023.100082

[13] Liu, Q. S., Zheng, T., Wang, P., Jiang, J. P., & Li, N. (2010). Adsorption isotherm, kinetic and mechanism studies of some substituted phenols on activated carbon fibers. *Chemical engineering journal*, *157*(2-3), 348-356, https://doi.org/10.1016/j.cej.2009.11.013

[14] Eddy, N. O., Ebenso, E. E. (2008). Adsorption and inhibitive properties of ethanol extracts of *Musa sapientum* peels as a green corrosion inhibitor for mild steel in H_2SO_4.. *Afr. J. Pure Appl. Chem*, *2*(6), 046-054

[15] Khadom, A. A., Yaro, A. S., H. Kadum, A. A., AlTaie, A. S., & Y. Musa, A. (2009). The Effect of Temperature and Acid Concentration on Corrosion of Low Carbon Steel in Hydrochloric Acid Media. *American Journal of Applied Sciences*, 6(7), 1403–1409, https://doi:10.3844/ajassp.2009.1403.1409

[16] Akinbulumo, O. A., Odejobi, O. J., & Odekanle, E. L. (2020). Thermodynamics and adsorption study of the corrosion inhibition of mild steel by *Euphorbia heterophylla L.* extract in 1.5 M HCl. *Results in Materials*, *5*, 100074, https://doi.org/10.1016/j.rinma.2020.100074

[17] Nwabanne, J. T., & Okafor, V. N. (2012). Adsorption and thermodynamics study of the inhibition of corrosion of mild steel in H_2SO_4 medium using *Vernonia amygdalina*. *Journal of Minerals and Materials Characterization and engineering*, *11*(09), 885

[18] Ostovari, A., Hoseinieh, S. M., Peikari, M., Shadizadeh, S. R., & Hashemi, S. J. (2009). Corrosion inhibition of mild steel in 1 M HCl solution by henna extract: A comparative study of the inhibition by henna and its constituents (Lawsone, Gallic acid, α-D-glucose, and Tannic acid). *Corrosion Science*, *51*(9), 1935-1949, https://doi.org/10.1016/j.corsci.2009.05.024

[19] Fouda, A. S., Megahed, H. E., Fouad, N., & Elbahrawi, N. M. (2016). Corrosion inhibition of carbon steel in 1 M hydrochloric acid solution by aqueous extract of *Thevetia peruviana*. *Journal of Bio-and Tribo-Corrosion*, *2*, 1-13, https://doi.org/10.1007/s40735-016-0046-z

[20] Chung, I. M., Malathy, R., Kim, S. H., Kalaiselvi, K., Prabakaran, M., & Gopiraman, M. (2020). Ecofriendly green inhibitor from Hemerocallis fulva against aluminum corrosion in sulphuric acid medium. *Journal of Adhesion Science and Technology*, 1–24. https://doi.org/10.1080/01694243.2020.1712770

[21] Husaini, M., & Ibrahim, M. B. (2020). Investigation of inhibition potential effect of organic compound for the corrosivity of phosphoric acid on aluminium. *International Journal of Engineering and Manufacturing*, 10(1), 41. https://doi.org/10.5815/ijem.2020.01.04

[22] Arukalam, I. O., Madufor, I. C., Ogbobe, O., & Oguzie, E. E. (2015). Inhibition of mild steel corrosion in sulfuric acid medium by hydroxyethyl cellulose. *Chemical Engineering Communications*, 202(1), 112–122. https://doi.org/10.1080/00986445.2013.838158

[23] Akatyev, N., & Samigolla, A. (2024). Sun protection properties and photostability of aqueous extracts of dandelion (*Taraxacum officinale L.*). *Prospects in Pharmaceutical Sciences*, 22(4), 160–167. https://doi.org/10.56782/pps.285

[24] Tsygankova, L. E., Vigdorovich, V. I., Shel, N. V., & Dubinskaya, E. V. (2013). Peculiarities of protective efficiency of nitrogen-containing inhibitors of steel corrosion. *International Journal of Corrosion and Scale Inhibition*, 2(4), 304–310.

[25] Solmaz, R., Kardaş, G., Yazıcı, B., & Erbil, M. (2008). Adsorption and corrosion inhibitive properties of 2-amino-5-mercapto-1,3,4-thiadiazole on mild steel in hydrochloric acid media. *Colloids and Surfaces A: Physicochemical and Engineering Aspects*, *312*(1), 7-17, https://doi.org/10.1016/j.colsurfa.2007.06.035